

## Synthesis, structural and electrochemical properties of Ni-rich material prepared by a sol-gel method

Mai Thanh Tung\*, Vu Duc Luong

*Department of Electrochemistry and Corrosion Protection, School of Chemical Engineering  
Hanoi University of Science and Technology, Hanoi, Vietnam*

Received 26 July 2016; Accepted for publication 19 December 2016

### Abstract

We report on a novel synthetic method of sol-gel processing to prepare Ni-rich cathode materials. We also studied and reported on the electrochemical properties of the resultant products. XRD revealed that a single phase Ni-rich powder can be synthesized by sol-gel processing. The Ni-rich material obtained has a high electrochemical capacity and good cycle ability. These results indicate that sol-gel processing is a promising method for preparing Ni-rich cathode materials. The sample prepared under the optimal conditions had a well ordered hexagonal layered structure. The charge-discharge tests showed that the initial capacities of the sample were 220.456 and 185.937 mAhg<sup>-1</sup> at the discharge rate of 0.1 C between 3.0 and 4.3 V, respectively. The capacity retention ratio was 81.36 % at 1 C after 50 cycles.

**Keywords.** Lithium-ion battery, cathode material, LiNi<sub>0.8</sub>Co<sub>0.1</sub>Mn<sub>0.1</sub>O<sub>2</sub>, sol-gel.

### 1. INTRODUCTION

Lithium cobalt oxide (LiCoO<sub>2</sub>), initially introduced in 1980, has been one of the most widely used positive electrode material in commercial lithium-ion batteries due to its high working voltage, reasonable cycle-life (300-500 cycles), and its easy preparation [1-3]. However, its high cost, toxicity, and the thermal instability of Li<sub>x</sub>CoO<sub>2</sub> phases limit its further use in newly developed multifunctional portable devices and electric vehicle systems [4].

LiNiO<sub>2</sub> is one of the most attractive next-generation cathode-material candidates for lithium-ion batteries (LIBs) because its reversible capacity is higher and its cost is lower than those of LiCoO<sub>2</sub> [2,3,5,6]. However, LiNiO<sub>2</sub> suffers from an intrinsic poor thermal stability in its fully charged state and a poor cycle life, both of which are related to the chemical and structural instability of tetravalent nickel. Comparatively, Ni-rich layered LiNi<sub>1-x-y</sub>Mn<sub>x</sub>Co<sub>y</sub>O<sub>2</sub>, wherein the composition of Ni is dominant over the Co and Mn, is a promising material because of a lower cost, less toxicity, an improved thermal stability, a sound cycling stability, and safety [7]. In these materials, layered LiNi<sub>0.8</sub>Co<sub>0.1</sub>Mn<sub>0.1</sub>O<sub>2</sub> has been intensively studied as a potential positive active electrode for application in plug-in hybrid electric vehicles (P-HEVs) [8-11].

The LiNi<sub>0.8</sub>Co<sub>0.1</sub>Mn<sub>0.1</sub>O<sub>2</sub> solid solution was initially synthesized by the conventional method such as solid-state method. However this method involves very high temperatures for a prolonged period of time with intermediated grinding, this led to problems with poor stoichiometry control, non-homogeneity.

In recent years, low temperature wet chemistry methods of synthesizing cathode active materials have gained importance because they do not have above problems and produce material with homogeneous distribution and high surface area. In addition, this technique makes possible the synthesis of nanosized particles, which has two advantages: it increases the effective surface area of the powder with the electrolyte and it increases the lithium intercalation efficiency by reducing the electron path inside the material that has a poor electronic conductivity [12]. In the case of Ni-rich cathode material, several low temperature methods like sol-gel and combustion methods have been reported [13, 14].

In this work, we report the sol-gel synthesis Ni-rich LiNi<sub>0.8</sub>Co<sub>0.1</sub>Mn<sub>0.1</sub>O<sub>2</sub> material. The effects of varying each initial condition on the structure, morphology, and electrochemical performances of the Ni-rich cathode material were investigated and the details are discussed in this paper.

## 2. EXPERIMENTAL

### 2.1. Material synthesis

The cathode material  $\text{LiNi}_{0.8}\text{Co}_{0.1}\text{Mn}_{0.1}\text{O}_2$  was synthesized by sol-gel method. Stoichiometric amounts of lithium acetate, nickel acetate, manganese acetate and cobalt acetate in a cationic ratio  $\text{Li}:\text{Ni}:\text{Co}:\text{Mn} = 1.05:0.8:0.1:0.1$  (with 5 % excess of lithium source) were dissolved in distilled water and mixed with an aqueous solution of acid acetic. The mixture was stirred for 24 h at room temperature. The solution was evaporated under continuous stirring at 80 °C until the viscosity green aquogel was formed. After drying at 120 °C in a drying oven overnight, the xerogel was crushed, subsequently heated at 480 °C for 4 h in oxygen atmospheric to decompose the organic constituents and nitrate components. The sample was then grounded, pelletized and calcined at 800 °C for 16 h under oxygen atmosphere. After being cooled to room temperature, the  $\text{LiNi}_{0.8}\text{Co}_{0.1}\text{Mn}_{0.1}\text{O}_2$  material was obtained.

### 2.2. Material characterization

The crystal structures of the  $\text{LiNi}_{0.8}\text{Co}_{0.1}\text{Mn}_{0.1}\text{O}_2$  material was characterized by an X-ray diffraction (XRD) measurement for which a Rigaku D Max/2000 PC with a  $\text{CuK}_\alpha$  radiation in the  $2\theta$  range of 10° to 80° was used at a scanning rate of 4°min<sup>-1</sup>. The particle morphology and elemental composition of the powders were analyzed using SEM, whereby the Hitachi S-4800 was equipped with an energy dispersive spectroscopy (EDS, OXFORD 7593-H) capability.

### 2.3. Electrochemical measurements

The electrochemical performances of the

$\text{LiNi}_{0.8}\text{Co}_{0.1}\text{Mn}_{0.1}\text{O}_2$  material was measured by using the CR2016 coin-type cells. To ensure a high electronic conductivity, 80:10:10 (wt.%) mixture of active material, polyvinylidenedifluoride (PVdF) as a binder and super P carbon as a conduction material respectively was grinded in a mortar. About 3 mg of the mixture were pressed with 90 MPa (5 t at  $\varnothing$  13 mm) on aluminium mesh and dried for 24 h in a vacuum oven at 110 °C. Lithium metal was used as an anode electrode, and a microporous-polyethylene separator was inserted between the cathode and the counter electrode and 1molL<sup>-1</sup>  $\text{LiPF}_6$  in an ethylene carbonate (EC) and dimethyl carbonate (DMC) mixture in the ratio EC:DMC (1:1) as electrolyte. All of the coin-type cells were prepared in an Ar-filled glove box in which the oxygen and moisture contents were controlled below 2.0 ppm. The cells were galvanostatically charged and discharged at 25 °C in the voltage range 3-4.3 V.

## 3. RESULTS AND DISCUSSION

Figure 1 displayed the XRD patterns of the  $\text{LiNi}_{0.8}\text{Co}_{0.1}\text{Mn}_{0.1}\text{O}_2$  cathode material. The XRD patterns of the sample showed sharp and clear doublet-peak splits of (006)/(102) and (108)/(110), indicating that samples comprising a well-ordered crystalline structure were formed. All reflections are indexed in agreement with the rhombohedral  $\alpha\text{-NaFeO}_2$  structure R3m and distinct impurity phases were not found in any of this pattern [15]. The unit-cell parameters were estimated and the results are summarized in table 1. Generally, the  $c/a$  value is employed to examine a layered material, for example, the  $c/a$  value of the material with an ideal cubic close layered structure is over 4.899 [16]. The refinement converged with lattice parameters  $a = 2.8378 \text{ \AA}$ ,  $c = 14.2019 \text{ \AA}$  and  $c/a = 5.004$ . This large value of  $c/a$  gives evidence of a well-ordered rhombohedral structure [15].

Table 1: The lattice parameters and the intensity ratios of the (003)/(104) and [(006) + (102)]/(101) for all samples

Sample name	a	c	c/a	$R_w$	$R_f$
$\text{LiNi}_{0.8}\text{Co}_{0.1}\text{Mn}_{0.1}\text{O}_2$	2.8378	14.2019	5.004	1.4018	0.5833

It has been reported that the intensity ratio of  $I_{(003)}/I_{(104)}$  reflects the cation mixing degree of the layered structure. In general, the value of  $I_{(003)}/I_{(104)}$  over 1.2 is an indication of small cation mixing [17, 18]. From table 1, the  $I_{003}/I_{104}$  ratio of the  $\text{LiNi}_{0.8}\text{Co}_{0.1}\text{Mn}_{0.1}\text{O}_2$  sample is 1.4 which is greater than 1.2, indicating a low cation disorder between the  $\text{Li}^+$  and  $\text{Ni}^{2+}$  of the  $\text{LiNi}_{0.8}\text{Co}_{0.1}\text{Mn}_{0.1}\text{O}_2$  samples.

The SEM picture of the  $\text{LiNi}_{0.8}\text{Co}_{0.1}\text{Mn}_{0.1}\text{O}_2$  sample was shown in Fig. 2. The as-prepared  $\text{LiNi}_{0.8}\text{Co}_{0.1}\text{Mn}_{0.1}\text{O}_2$  powder has well developed regular particles of quasi-spherical shape with a diameter distribution in the range 500-1000 nm, similar to previously reported SEM images [19]. The fast hydrolysis reaction causes micelles to appear rapidly. These rapidly produced micelles are very

easy to coagulate each other upon their appearance and to form gel quickly. So the micelles do not have enough time to grow separately but reunite together easily. This can be the reason why  $\text{LiNi}_{0.8}\text{Co}_{0.1}\text{Mn}_{0.1}\text{O}_2$  powder has a small particle size but serious agglomeration.

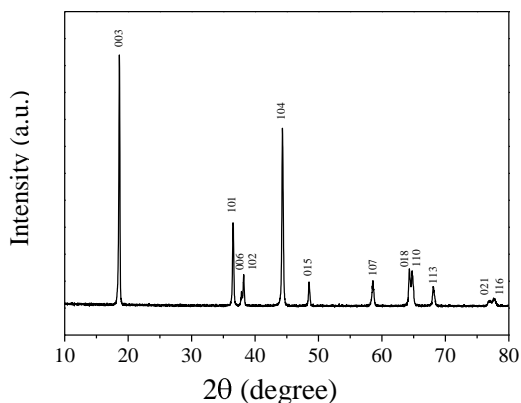


Figure 1: XRD patterns of the  $\text{LiNi}_{0.8}\text{Co}_{0.1}\text{Mn}_{0.1}\text{O}_2$  sample

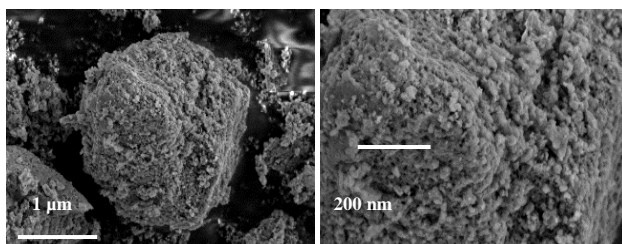


Figure 2: SEM images of as-prepared  $\text{LiNi}_{0.8}\text{Co}_{0.1}\text{Mn}_{0.1}\text{O}_2$  powder

The electrochemical performance of  $\text{LiNi}_{0.8}\text{Co}_{0.1}\text{Mn}_{0.1}\text{O}_2$  layered material was examined at 25 °C by charge/discharge and cyclic voltammetry (CV) studies. Fig. 3a displayed the charge–discharge curves as measured during galvanostatic cycling with potential limitation of  $\text{LiNi}_{0.8}\text{Co}_{0.1}\text{Mn}_{0.1}\text{O}_2$  material at 0.1 C-rate was applied between 3 and 4.3 V vs.  $\text{Li}/\text{Li}^+$ . The first charge and discharge capacities of the  $\text{LiNi}_{0.8}\text{Co}_{0.1}\text{Mn}_{0.1}\text{O}_2$  material are about 220.456 and 185.937  $\text{mAhg}^{-1}$ . The cycling stabilities of the samples at a constant current density of 185.0  $\text{mAhg}^{-1}$  (1C rate) between 3.0 V and 4.3 V were also investigated and the results are shown in Fig. 3 (b). The first cycle discharge capacity was 161.395  $\text{mAhg}^{-1}$  and that of the 50<sup>th</sup> cycles was 131.729  $\text{mAhg}^{-1}$  with 81.36 % of capacity retention.

Rate capability is one of the most important electrochemical-performance measures of the LIBs that are required for high-power devices such as electric hybrid vehicles and power tools. The rate performance of  $\text{LiNi}_{0.8}\text{Co}_{0.1}\text{Mn}_{0.1}\text{O}_2$  prepared was

investigated between 3.0 and 4.3 V. The initial discharge curves of  $\text{LiNi}_{0.8}\text{Co}_{0.1}\text{Mn}_{0.1}\text{O}_2$  at different charge–discharge rates (0.1 C/0.1 C, 0.5 C/0.5 C, 0.5 C/1 C, 0.5 C/3 C, 0.5 C/4 C, 0.5 C/5 C, 0.5 C/7 C) are shown in Fig. 4(a). It can be seen that the profiles were similar to each other except the faster voltage drop with capacity fading at the higher C-rates, which can be attributed to the increased polarization of the electrodes at high current densities. The polarization increases with increasing current rate as a result of the reduced discharge time for lithium on intercalation into the crystal lattice, as only the surfaces of active materials participate in the reaction [16]. As shown in Fig (4b), for 0.1C, 0.5C, 1C, 3C, 4C, 5C, and 7C, the discharge capacities are 182  $\text{mAhg}^{-1}$ , 168  $\text{mAhg}^{-1}$ , 160  $\text{mAhg}^{-1}$ , 144  $\text{mAhg}^{-1}$ , 137  $\text{mAhg}^{-1}$ , 127  $\text{mAhg}^{-1}$ , and 110  $\text{mAhg}^{-1}$ . The curves demonstrated good rate capability when the C-rates increased from 0.1 C to 7 C, and excellent cycling performance was observed at each C-rate for three cycles. The similar phenomena were found when the C-rates decreased from 7 C to 0.1 C. The main reason for the capacity fading may result from

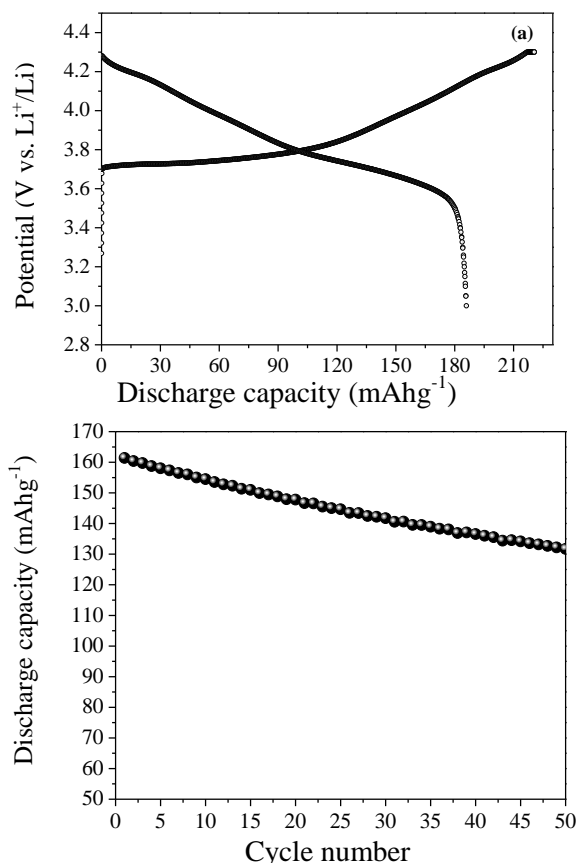
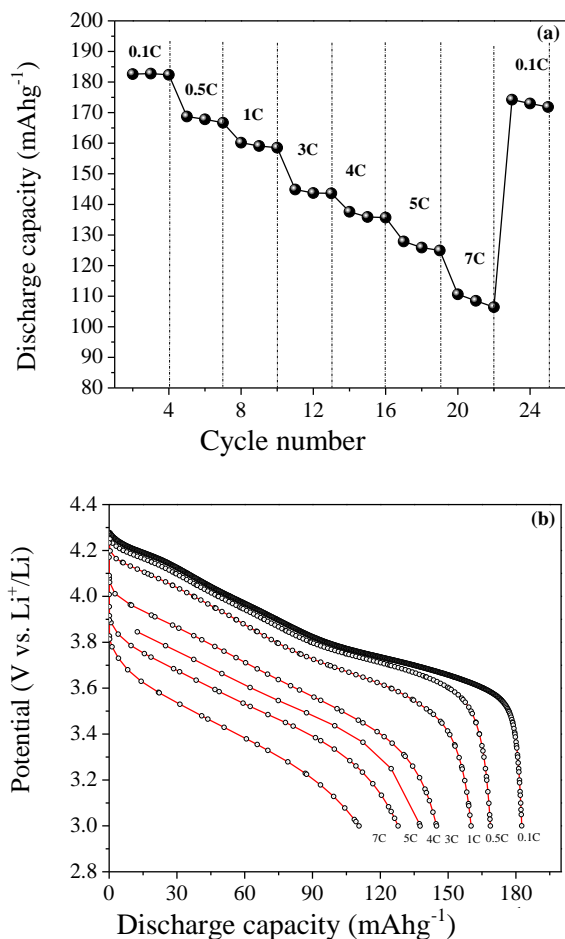


Figure 3: Electrochemical properties of samples in the voltage range of 3.0 V to 4.3 V at 25 °C: (a) Initial charge/discharge capacity at a rate of 0.1C, and (b) discharge capacity vs. cycle number at 1C.

the accumulation of lattice defects especially at a high charge and discharge rate, as well as the occurrence of irreversible structural phase transition which led to no enough sites for lithium ion intercalation.



**Figure 4:** Rate capability of the  $\text{LiNi}_{0.8}\text{Co}_{0.1}\text{Mn}_{0.1}\text{O}_2$  from  $18.5 \text{ mAg}^{-1}$  to  $129.5 \text{ mAg}^{-1}$  with potential limits of 3.0 V to 4.3 V (vs.  $\text{Li}^+/\text{Li}$ ) at room temperature: (a) specific discharge capacity, and (b) normalized capacity retention rate vs. 0.1C at different C rates

The cyclic voltammetry was carried out for  $\text{LiNi}_{0.8}\text{Co}_{0.1}\text{Mn}_{0.1}\text{O}_2$  to evaluate the reaction progress during charge–discharge experiment. Fig. 5 shows the cyclic voltammetry curves of  $\text{LiNi}_{0.8}\text{Co}_{0.1}\text{Mn}_{0.1}\text{O}_2$  electrode for initial three cycles. The profiles of the curves are similar except the positive scan for the first cycle, which can be attributed to the cation mixing. It's known that the cation mixing results in obvious irreversible capacity in the initial cycle, which corresponds to significantly reduced peak area in later cycle in the cyclic voltammetric curves. According to the literature [10, 20, 21] the peaks in the cyclic voltammetric curve demonstrate the phase transition along with lithium insertion and extraction.

When two phases were coexisted, one peak can be observed. As seen from the Fig. 5, three couples of peaks were found during the charge–discharge process in the second and third cycle. It has been reported that the three peaks occurred in the positive scan correspond to the transition of hexagonal phase ( $\text{H}_1$ ) to monoclinic phase (M), monoclinic phase (M) to hexagonal phase ( $\text{H}_2$ ), hexagonal phase ( $\text{H}_2$ ) to hexagonal phase ( $\text{H}_3$ ), respectively. Generally, phase transitions may result in capacity fading due to the irreversible change of the structure. In our work, the sample synthesized at the optimal conditions exhibited excellent cycling performance, as confirmed by the almost overlapping cyclic voltammetric curves during discharge process.

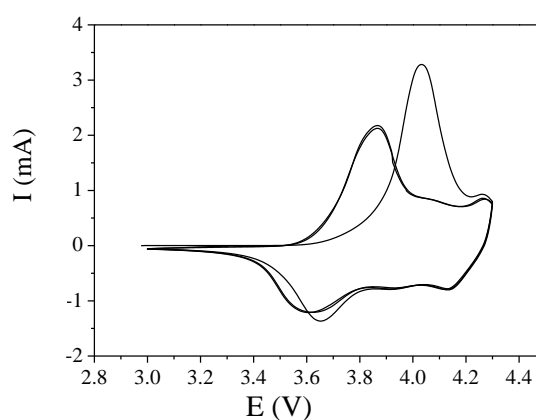


**Figure 5:** Cyclic voltammetry of LNMC sample with  $0.1 \text{ mVs}^{-1}$  in a range of 3.0–4.3 V

#### 4. CONCLUSION

In summary, we have successfully synthesized highly crystalline layered  $\text{LiNi}_{0.8}\text{Co}_{0.1}\text{Mn}_{0.1}\text{O}_2$  cathode material by conventional sol–gel method. The obtained product develops a well-ordered rhombohedral structure with high  $c/a$  and low cation mixing. The structure and morphology of this sample was investigated as a function of the cycling in the voltage range 3.0–4.3 V. In addition, cyclic voltammetric tests demonstrated that there are three reversible phase transitions involved in the charge–discharge process

**Acknowledgement.** This work was supported by the Nippon Sheet Glass Foundation for Materials Science and Engineering and Ministry of Science and Technology (Vietnam Taiwan Protocol Project 2016).

#### REFERENCES

1. Armand M. *Issues and Challenges Facing Rechargeable Lithium Batteries*, Nature, **414**

- (November), 359-367 (2001).
- Ellis B. L., Lee K. T., Nazar L. F. *Positive Electrode Materials for Li-Ion and Li-Batteries*, Chem. Mater., **22(3)**, 691-714 (2010).
  - Goodenough J. B., Kim Y. *Challenges for Rechargeable Li Batteries*, Chem. Mater., **22(3)**, 587-603 (2010).
  - Amatucci G. *Cobalt Dissolution in LiCoO<sub>2</sub>-Based Non-Aqueous Rechargeable Batteries*. Solid State Ionics, **83(1-2)**, 167-173 (1996).
  - Ohzuku T., Ueda A., Nagayama M., Iwakoshi Y., Komori H. *Comparative Study of LiCoO<sub>2</sub>, LiNi<sub>1/2</sub>Co<sub>1/2</sub>O<sub>2</sub> and LiNiO<sub>2</sub> for 4 Volt Secondary Lithium Cells*, Electrochim. Acta, **38(9)**, 1159-1167 (1993).
  - Park G. D., Chan Kang Y. *Characteristics of Precursor Powders of a Nickel-Rich Cathode Material Prepared by a Spray Drying Process Using Water-Soluble Metal Salts*, RSC Adv., **4(83)**, 44203-44207 (2014).
  - Luo D., Li G., Fu C., Zheng J., Fan J., Li Q., Li L. *LiMO<sub>2</sub> (M = Mn, Co, Ni) Hexagonal Sheets with (101) Facets for Ultrafast Charging-discharging Lithium Ion Batteries*, J. Power Sources, **276**, 238-246 (2015).
  - Saavedra-Arias J. J., Karan N. K., Pradhan D. K., Kumar A., Nieto S., Thomas R., Katiyar R. S. *Synthesis and Electrochemical Properties of Li(Ni<sub>0.8</sub>Co<sub>0.1</sub>Mn<sub>0.1</sub>)O<sub>2</sub> Cathode Material: Ex Situ Structural Analysis by Raman Scattering and X-Ray Diffraction at Various Stages of Charge-discharge Process*, J. Power Sources, **183(2)**, 761-765 (2008).
  - Lu H., Zhou H., Svensson A. M., Fossdal A., Sheridan E., Lu S., Vullum-Bruer F. *High Capacity Li(Ni<sub>0.8</sub>Co<sub>0.1</sub>Mn<sub>0.1</sub>)O<sub>2</sub> Synthesized by sol-gel and Co-Precipitation Methods as Cathode Materials for Lithium-Ion Batteries*, Solid State Ionics, **249-250**, 105-111 (2013).
  - Eom J., Kim M. G., Cho J. *Storage Characteristics of Li(Ni<sub>0.8</sub>Co<sub>0.1+x</sub>Mn<sub>0.1-x</sub>)O<sub>2</sub> (x=0, 0.03, and 0.06) Cathode Materials for Lithium Batteries*, J. Electrochem. Soc., **155(3)**, A239 (2008).
  - Zhang B., Li L., Zheng J. *Characterization of Multiple Metals (Cr, Mg) Substituted Li(Ni<sub>0.8</sub>Co<sub>0.1</sub>Mn<sub>0.1</sub>)O<sub>2</sub> Cathode Materials for Lithium Ion Battery*, J. Alloys Compd., **520**, 190-194 (2012).
  - Kim S.-B., Kim S. -J., Kim C.-H., Kim W.-S., Park, K.-W. *Nanostructure Cathode Materials Prepared by High-Energy Ball Milling Method*, Mater. Lett., **65(21-22)**, 3313-3316 (2011).
  - Ahn W., Lim S. N., Jung K.-N., Yeon S.-H., Kim K.-B., Song H. S., Shin K.-H. *Combustion-Synthesized Li(Ni<sub>0.6</sub>Co<sub>0.2</sub>Mn<sub>0.2</sub>)O<sub>2</sub> as Cathode Material for Lithium Ion Batteries*, J. Alloys Compd., **609**, 143-149 (2014).
  - Ting-Kuo Fey G., Chen J.-G.; Wang Z.-F., Yang H.-Z., Prem Kumar T. *Saturated Linear Dicarboxylic Acids as Chelating Agents for the Sol-gel Synthesis of LiNi<sub>0.8</sub>Co<sub>0.2</sub>O<sub>2</sub>*, Mater. Chem. Phys., **87(2-3)**, 246-255 (2004).
  - Vu D.-L., Lee J. *Properties of Li(Ni<sub>0.8</sub>Co<sub>0.1</sub>Mn<sub>0.1</sub>)O<sub>2</sub> as a High Energy Cathode Material for Lithium-Ion Batteries*, Korean J. Chem. Eng., **32(4)**, 1-13 (2015).
  - Karthikeyan K., Amaresh S., Lee G. W., Aravindan V., Kim H., Kang K. S., Kim W. S., Lee Y. S. *Electrochemical Performance of Cobalt Free, Li<sub>1.2</sub>(Mn<sub>0.32</sub>Ni<sub>0.32</sub>Fe<sub>0.16</sub>)O<sub>2</sub> Cathodes for Lithium Batteries*, Electrochim. Acta, **68**, 246-253 (2012).
  - Zhang X., Jiang W. J., Mauger A., Gendron F., Julien C. M. *Minimization of the Cation Mixing in Li<sub>1+x</sub>(NMC)<sub>1-x</sub>O<sub>2</sub> as Cathode Material*, J. Power Sources, **195(5)**, 1292-1301 (2010).
  - Huang Z., Gao J., He X., Li J., Jiang C. *Well-Ordered Spherical LiNi<sub>x</sub>Co<sub>(1-2x)</sub>Mn<sub>x</sub>O<sub>2</sub> Cathode Materials Synthesized from Cobalt Concentration-Gradient Precursors*, J. Power Sources, **202**, 284-290 (2012).
  - Lu H., Zhou H., Svensson A. M., Fossdal A., Sheridan E., Lu S., Vullum-Bruer F. *High Capacity Li(Ni<sub>0.8</sub>Co<sub>0.1</sub>Mn<sub>0.1</sub>)O<sub>2</sub> Synthesized by Sol-gel and Co-Precipitation Methods as Cathode Materials for Lithium-Ion Batteries*, Solid State Ionics, **249-250**, 105-111 (2013).
  - Liu K., Yang G.-L., Dong Y., Shi T., Chen L. *Enhanced Cycling Stability and Rate Performance of Li(Ni<sub>0.5</sub>Co<sub>0.2</sub>Mn<sub>0.3</sub>)O<sub>2</sub> by CeO<sub>2</sub> Coating at High Cutoff Voltage*, J. Power Sources (2014).
  - Chen Y., Zhang Y., Chen B., Wang Z., Lu C. *An Approach to Application for Li(Ni<sub>0.6</sub>Co<sub>0.2</sub>Mn<sub>0.2</sub>)O<sub>2</sub> Cathode Material at High Cutoff Voltage by TiO<sub>2</sub> Coating*, J. Power Sources, **256**, 20-27 (2014).

Corresponding author: **Mai Thanh Tung**

Department of Electrochemistry and Corrosion Protection  
 School of Chemical Engineering  
 Hanoi University of Science and Technology, Hanoi, Vietnam  
 No 1, Dai Co Viet, Ha Ba Trung, Hanoi  
 E-mail: tung.maithanh@hust.edu.vn.